Anal. Bioanal. Electrochem., Vol. 14, No. 11, 2022, 1044-1059

Analytical & Bioanalytical Electrochemistry

2022 by CEE
www.abechem.com

Full Paper

The Influence of Olive Leaves Extract as An Eco-Friendly Inhibitor, Temperature, and Immersion Time on Tin Corrosion Behavior in 3wt% Acetic Acid using Response Surface Methodology

Sara Lahmady and Issam Forsal*

Laboratory of Engineering and Applied Technologies, School of Technology, Beni Mellal, Morocco

*Corresponding Author, Tel.: +212661118208

E-Mail: forsalissam@yahoo.fr

Received: 9 October 2022 / Received in revised form: 15 November 2022 / Accepted: 21 November 2022 / Published online: 30 November 2022

Abstract- Metal packaging is excellent for storing canned foods. However, due to the acidic nature of the canning solution, the contact of the food with the metal container diminishes its shelf life, and can produce a corrosion problem. The inhibiting effect of olive leaves extract on tin corrosion in 3 wt% acetic acid was examined in this study. The impact of the concentration of inhibitor (0.1–1g/L), immersion time (0.5–12h), and temperature (20–50°C) were investigated employing a statistical approach based on the design of experiment (DOE). For those three factors, response surface methodology (RSM) using face-centered central composite design (FCCD) was chosen and applied to the design matrix. A potentiodynamic polarization (PDP) test was used to assess the output corrosion current density (i_{corr}) under various conditions specified in the design matrix. The model proved correct with a good coefficient of determination of (R^2 = 97.84%). The outcomes of the PDP method demonstrate that the corrosion current density rises with temperature, indicating that physisorption is the dominant mechanism.

Keywords- Tin corrosion; Metal packaging; Acetic acid; Face-centered central composite design; Response surface methodology

1. INTRODUCTION

Metal packaging preserves the physical, chemical, and organoleptic qualities of the food product, it also extends its shelf life and ensures safe consumption [1,2]. As known, tinplate is the most important coated steel used in food and beverage metal packaging applications due to its impermeability, formability, solderability, and low cost [3]. Tinplate is a heterogeneous material with a layered structure, approximately 1 μm of tin layer is electrolytically deposited (electrolytic tinplate (ETP)) on cold-rolled low carbon steel (0.003-0.12% carbon) (ITRI 2000) [4–6]. For this material, tin offers corrosion resistance, manufacturing lubricity, a gleaming look, and a benign food contact surface, while steel provides toughness and formability [7].

However, there are substantial issues associated with the usage of tinplate, such as interior corrosion caused by the interaction of the metallic substance with the can contents, particularly acidic foodstuffs [8]. This problem causes migration of tin to the food, loss of quality and purity of the processed items [8,9]. The contamination of food by tin can render it unsafe for consumption if the concentration of this metal exceeds the tolerated limits. The EU regulation 1881/2006 set maximum limits for tin (inorganic tin) at 200 mg/kg for canned food other than beverages, 100 mg/kg for canned beverages [9]. Based on certain studies, tin concentrations exceeding 200 mg/kg cause gastrointestinal disturbances, with symptoms including nausea, gastric discomfort, and vomiting [8,10].

According to the literature, the corrosion of metal packaging is affected by a variety of factors, including the product's composition (acidic, sulfur, and/or salty foods...), storage conditions (degree of vacuum, duration, temperature), and the existence of corrosion accelerators present in food (O_2, anthocyanins, nitrates, sulphides, etc.) [11–14].

To reduce the risk of tin contamination in foods, one of the most commonly used coatings in the food canning industry are lacquers containing significant amounts of organic solvents, up to 80% of the total weight [4]. However, the lacquer has some flaws, including adhesion failure and organic contaminant migration [15,16]. As a result, there is currently a lot of interest in the usage of various types of environmentally friendly and low-cost corrosion inhibitors [4]. Some compounds have already been described as eco-friendly and efficient corrosion inhibitors that prevent the dissolution of tin under various conditions. For example, three cyclic amino acids (Histidine, Tyrosine, and Phenylalanine) have been utilized to inhibit tin corrosion in 2% NaCl at pH (2 and 5) [17].In another work, pectin obtained from low-cost tomato peel waste (TPP) exhibited good inhibitory efficiency against tin surface corrosion in a test solution containing sodium chloride and acetic acid [4]. Brahim EL Ibrahimi et al. investigated the inhibitory impact of proline (Pro) amino acid on tin in acidic (pH = 2) and near-neutral (pH = 5) environments, discovering that (Pro) has a remarkable inhibition efficacy of over 65% at pH 5 [11].

According to the views expressed previously, the interest of this investigation is to understand the effect of olive leaf extract as a green corrosion inhibitor, as well as the impact

of temperature and immersion time on the corrosion of tin in contact with an aggressive acid solution (acetic acid CH_3COOH). Response surface methodology (RSM) with face-centered central composite design (FCCD) was adopted to investigate the combined effects of these three parameters. RSM is a mathematical and statistical method that is used to examine the individual and interactional influences of variables on responses [18]. It is typically fitted using polynomial equations [18]. A potentiodynamic polarization test was performed to evaluate the output corrosion current density (i_{corr}) under various design matrix conditions. The impacts of different control factors on (i_{corr}) are precisely analyzed using a regression equation. This equation was then validated utilizing analysis of variance (ANOVA).

2. EXPERIMENTAL METODS

2.1. Preparation of inhibitor and corrosive medium

Fresh olive leaves were harvested from Beni Mellal region, Morocco, in March. Olive leaves were rinsed with tap water to remove contaminants and dried for 15 days in the shade at room temperature (23°C- 27 °C), before being pulverized into powder. The extraction was performed using the maceration method in methanol. 10 g of olive leaves powder was added to 200 mL of methanol with stirring for 48 hours. Following that, the extract was concentrated in a rotary evaporator and stored in an opaque sterile container.

Acetic acid (CH_3COOH) was chosen for this study to simulate an aggressive acid condition prevalent in canned food products; this solution is commonly employed for the preservation or as an acidity regulator [19]. A 3 wt% CH_3COOH solution (blank solution) was made by diluting acetic acid (>99%) from Sigmaaldrich with distilled water.

2.2. Preparation of metal specimens

The working electrode was composed of pure tin, with an exposed surface area of 0.5 cm^2. Prior to each experiment, the surface of the electrode was polished using several grades (1200, 1500, and 2000) of grit silicon carbide (SiC) emery papers. It is degreased with acetone, washed thoroughly with distilled water, and dried with warm air.

2.3. Response surface methodology and face-centered central composite design (FCCD)

The number of potentiodynamic tests necessary to evaluate the effect of three parameters (inhibitor concentration, temperature, and immersion time) on the corrosion current density of tin in 3wt% acetic acid can be very high using a traditional approach. The Response Surface Methodology (RSM) is one of the most prominent statistical approaches that can be very useful in reducing the number of tests [20–22]. RSM offers reliability and process optimization with a good prognosis for predictive model innovation [20]. Response surfaces are graphical presentations of the interactive impacts of independent variables on responses or dependent

variables. This method is effective for examining the effect of these factors and their interactions with each other [23].

In this examination, the full quadratic model (second order polynomial) is adopted to demonstrate linear interactions and the quadratic effect of process factors on response. This mathematical model is represented by Equation (1) [24]:

$$\boldsymbol{Y = b_0 + \sum_i^k b_i X_i + \sum_{i=1}^{k-1} \sum_{j=i+1}^{k} b_{ij} X_i X_{ij} + \sum_{i=1}^{k} b_{ii} X^2{}_i} \quad \textbf{(1)}$$

The quadratic response for three independent variables of X_1, X_2, and X_3 is represented in Equation (2) below [24]:

$$\mathbf{Y} = \boldsymbol{b_0 + b_1 X_1 + b_2 X_2 + b_3 X_3 + b_{12} X_1 X_2 + b_{13} X_1 X_3 + b_{23} X_2 X_3 + b_{11} X_1^2 + b_{22} X_2^2 + b_{33} X_3^2} \quad \textbf{(2)}$$

where:

Y: Response of current density (i_{corr}).

$\boldsymbol{X_1}$ $\boldsymbol{X_2}$, and $\boldsymbol{X_3}$: Independent parameters were signifying the inhibitor concentration, temperature, and immersion time.

$\boldsymbol{b_0}$: constant. $\boldsymbol{b_1}$, $\boldsymbol{b_2}$, and $\boldsymbol{b_3}$: constants reflected the influence of parameters $\boldsymbol{X_1}$, $\boldsymbol{X_2}$, and $\boldsymbol{X_3}$.

$\boldsymbol{b_{12}}$, $\boldsymbol{b_{13}}$, $\boldsymbol{b_{23}}$: Constants represented the relationship between the two factors $\boldsymbol{X_1X_2}$, $\boldsymbol{X_1X_3}$, $\boldsymbol{X_2X_3}$.

$\boldsymbol{b_{11}}$, $\boldsymbol{b_{22}}$, and $\boldsymbol{b_{33}}$: Constants were representing the effect of quadratic $\boldsymbol{X_1}$ $\boldsymbol{X_2}$, and $\boldsymbol{X_3}$.

In RSM, different designs can be utilized; the diversity between these designs is defined by the number of trials and the experiment points selected [23]. Face-centered central composite design (FCCD) is one of the RSM techniques that uses a five-level design by introducing a coefficient (α) called star points. This method is quite beneficial and commonly utilized for fitting a full quadratic model [25,26].

As previously stated, this article uses a (FCCD) to investigate the influence of the concentration of olive leaves extract as an inhibitor (X_1), temperature (X_2), and immersion time (X_3). The effect of experimental conditions on the corrosion current density (i_{corr}) was studied using a three-factor, three-level (FCCD) as shown in Table 1.

Table 1. Levels of experimental factors selected for the FCCD

Parameter	**Symbol**	**Unit**	**Level of parameters**		
			Low (-1)	**Center (0)**	**High (1)**
Inhibitor concentration	X_1	**(g/L)**	0.1	0.55	1
Temperature	X_2	**(°C)**	20	35	50
Immersion time	X_3	**(h)**	0.5	6.25	12

The numerical values are coded such that the minimum corresponds to -1 and the maximum corresponds to +1; these are known as factorial points. The middle of the maximum and

minimum is 0 and is known as the center point, which plays an important function since they help to reduce model error and determine the actual direction of the curve through the curvature [25]. The software in the FCCD approach examines other points (star points) by introducing an alpha coefficient, these points in the axial part of the study domain are at (+α,0), (-α,0), (0,+ α), (0,- α) [26,27]. Figure 1 illustrates a schematic representation of FCCD design in which is a cube with axial points on the face centers (α=1) in this case [27].

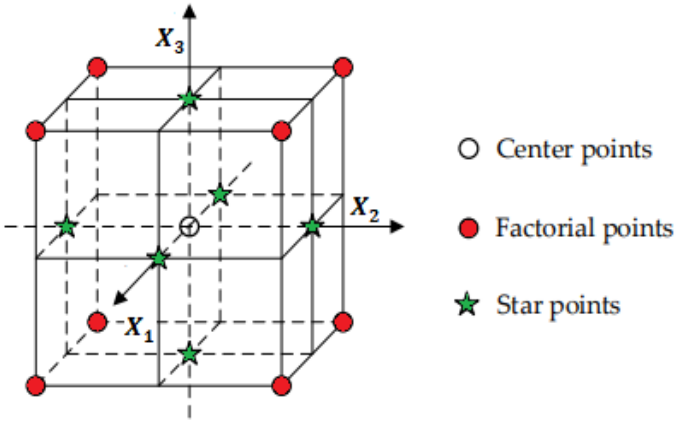

Figure 1. Schematic representation of FCCD design with the position of several points including center, factorial, and star points

Table 2. Experimental design based on the FCCD design matrix for the three variables

	Coded values			**Real values**		
Experiments	**X_1**	**X_2**	**X_3**	**Inhibitor concnetration**	**Temperature**	**Immersion time**
1	0	0	0	0.55	35	6.25
2	0	0	-1	0.55	35	0.5
3	-1	1	1	0.1	50	12
4	1	1	1	1	50	12
5	0	0	1	0.55	35	12
6	0	-1	0	0.55	20	6.25
7	-1	-1	-1	0.1	20	0.5
8	1	-1	1	1	20	12
9	0	0	0	0.55	35	6.25
10	0	0	0	0.55	35	6.25
11	-1	1	-1	0.1	50	0.5
12	1	0	0	1	35	6.25
13	0	1	0	0.55	50	6.25
14	-1	0	0	0.1	35	6.25
15	-1	-1	1	0.1	20	12
16	1	-1	-1	1	20	0.5
17	0	0	0	0.55	35	6.25
18	0	0	0	0.55	35	6.25
19	0	0	0	0.55	35	6.25
20	1	1	-1	1	50	0.5

2.4. Design of experiment and design matrix

The design of experiment (DOE) was designed using JMP 16 software according to the testing interval. An experiment number of ($N = 2^k + 2k + n$) was needed for the RSM employing face-centered central composite design, where k is the number of independent variables and n runs experiments at the center point [26]. The experimental design includes 20 experimental runs, which are reported in Table 2, with 6 axial points, 6 center points, and 8 factorial points. Table 2 summarizes all of the experimental factors (inhibitor concentration, temperature, and immersion time) considered by DOE design. The results were entered into JMP 16 software for further analysis.

2.5. Conducting potentiodynamic polarization tests

All electrochemical experiments were conducted using a Potentiostat of type OrigaStat 100, controlled by Origamaster5 software. The cell used with three electrodes, consisting of working electrode (pure tin), a platinum electrode as counter electrode, and saturated calomel electrode (SCE) as a reference electrode. Open circuit potential (OCP) surveillance was performed by immersing the working electrode in the corrosive medium (3 wt% acetic acid) for 20 min (the time required to obtain steady state conditions) for each experiment.

The potentiodynamic polarization curves were performed on pure tin electrode by changing the potential from -750 to -100 mV (*vs.* SCE) using a scan rate of 1 mV/s. The Tafel extrapolation method was used to calculate the corrosion current density (i_{corr}). Each experiment was conducted in accordance with the process variable conditions indicated in the design matrix.

3. RESULTS AND DISCUSSION

3.1. Potentiodynamic polarization curves

The potentiodynamic polarization curves used to calculate the corrosion current density for the RSM with FCCD are shown in Figure 2.

The gained curves revealed that the examined factors (inhibitor concentration, temperature, and immersion time) have an influence on the current density value. According to the literature, tin, when dissolved as Sn^{2+} in an acidic solution, oxidizes quickly to Sn^{4+}. Further Sn^{4+} hydrolysis produces a very insoluble $Sn(OH)_4$, which can deposit on the tin surface and form a passive film [28]. The high acidic (pH = 3.5) solution used in this experiment caused the anodic, tin dissolving reaction with its passage from the metal surface into the solution [4], demonstrating that acetate ions and a low pH value play a key role in the corrosion behavior of tin.

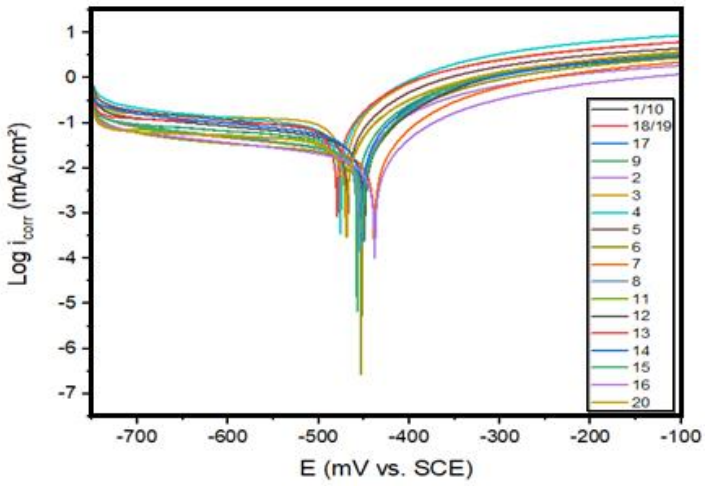

Figure 2. PDP curves of tin with variations in inhibitor concentration, temperature, and immersion time based on an experiment design of RSM with FCCD

3.2. Second-Order polynomial equation

A total of 20 runs of experiments were performed to obtain the responses of the dependent variable (corrosion current density). Table 3 displays the experimental design of the FCCD as well as the outcomes of the corrosion current density.

Table 3. Experimental and predicted data for response variables obtained from the FCCD

	Parameter			**Response i_{corr} (µA/cm²)**	
Experiment Run	**Inhibitor concnetration**	**Temperature**	**Immersion time**	**Experiment Observation**	**Predicted**
1	0.55	35	6.25	47.27	48.84
2	0.55	35	0.5	42.25	40.4
3	0.1	50	12	100.5	102.24
4	1	50	12	79.9	83.68
5	0.55	35	12	65.03	60.63
6	0.55	20	6.25	21.56	25.1
7	0.1	20	0.5	17.8	15.57
8	1	20	12	22.39	21.85
9	0.55	35	6.25	46.4	48.84
10	0.55	35	6.25	47.27	48.84
11	0.1	50	0.5	65.07	67.16
12	1	35	6.25	42.35	37.12
13	0.55	50	6.25	91.6	81.81
14	0.1	35	6.25	47	45.97
15	0.1	20	12	24.63	24.02
16	1	20	0.5	16.64	16.45
17	0.55	35	6.25	48.04	48.84
18	0.55	35	6.25	46.8	48.84
19	0.55	35	6.25	46.8	48.84
20	1	50	0.5	49.49	51.65

According to the data in Table 3, the minimum corrosion current density was obtained in experiment number 16, with a higher concentration of extract (1 g/L) and the lowest temperature and immersion time. Conversely, the higher corrosion rate was obtained in experiment 3, which was a combination of the lowest concentration of olive leaves extract (0.1 g/L) and the highest temperature and immersion duration of 50°C and 12 h, respectively. The results demonstrate that immersion time and temperature appear to have a negative impact, implying that increasing these two elements will increase corrosion current density and consequently the corrosion rate.

The corrosion current density was therefore evaluated by RSM using JMP 16 software to provide an empirical link between the response and the input variables. The regression equation (second-order polynomial) for corrosion current density obtained using FCCD is shown in the Equation 3 below in terms of uncoded parameters.

$$i_{corr}\ (\mu A/cm^2) = -2.5 + 52.9\ Inhibitor + 0.307\ Temp - 1.41\ Immersion - 36.0\ Inhibitor * Inhibitor + 0.0205\ Temp*Temp + 0.0505\ Immersion*Immersion - 0.607\ Inhibitor*Temp - 0.295\ Inhibitor*Immersion + 0.0772\ Temp*Immersion \quad (3)$$

The predicted outcomes presented in Table 3 were calculated using Equation (3). This mathematical model explains the linear and interaction influences of the process parameters on the (i_{corr}), as well as their quadratic effects. The reliability of the equation will be verified in the next sections.

3.3. Validity evaluation of the quadratic Model

The analysis of variance (ANOVA) is a common statistical method for determining the adequacy and the significance of the quadratic model, and it permits testing the influence of various parameters on the dependent variable (response) [29,30].

The standard $F_{critical}$ = F (9, 10, 0.05) =3.02 was employed in this investigation, where 9 represents the degree of freedom of model, 10 represents the degree of freedom of residual error, and 0.05 indicates the level of significance. Table 4 displays the (ANOVA) findings for the fitted equation. The calculated F value of the model was higher than the F critical value, indicating that it can reject the null hypothesis that all coefficients are zero and that the model is statistically significant [31,32]. When determining if the overall results are significant, the F statistic must be utilized in conjunction with the p-value. If the p-value is higher than the alpha level or risk degree (0.05), then the results are not significant and the null hypothesis cannot be rejected [31,33]. In our investigation, the confidence level (95%) was used, and the alpha level was set to be less than 0.05, indicating model validation. As a result, the p-value from this model's ANOVA is 0.000, indicating that there is a big difference between factors.

Table 4. Analysis of variance (ANOVA) for the regression equation

Source	Degree of Freedom	Adj. Sum of Square	Adj. Mean Square	F-Value	F critical	p-Value	Remarks
Model	9	9910.4	1101.16	50.36	3.02	0	Significant
Error	10	218.7	21.87	///	///	///	///
Lack-of-Fit	5	217.5	43.5	185.7	///	///	///
Pure Error	5	1.2	0.23	///	///	///	///
Total	19	10129					
R^2: 97.84%			R^2 (adj.): 95.90%			R^2 (pred.): 86.19%	

Furthermore, R^2 is 97.84%, indicating a good agreement between the experimental and predicted values of the output, with just 2.16% of the overall variation not accounted by the empirical model. The adjusted value (R^2 adj) is 95.90%, indicating that the independent factors are responsible for the overall variance of 4.1% in response. The results of the analysis and observations showed a good correlation between the experimental outcomes and the values predicted by the statistical model, demonstrating the model's efficacy.

3.4. The effects of extract concentration, temperature, and immersion time on the corrosion current density

To exactly determine the impact of each parameter on the corrosion current density, The Pareto chart in Figure 3 illustrates the standardized effects of extract concentration, temperature, and immersion duration on the corrosion current density (i_{corr}). The T-test can be used to determine whether a variable is statistically significant. It is used to estimate the amount and significance of the effects. Each bar in Pareto graph indicates a type of the factor's T-value; the height of the bar reflects the importance of the factor. As a result, temperature has the greatest influence on the corrosion rate of pure tin. The bars in Figure 3 depict the parameters temperature, immersion time, inhibitor concentration, interaction BC, interaction AB, and the quadratic effect of factor A crossing the reference line at 2.23. According to this fitted model, these factors are statistically significant at the 0.05 level.

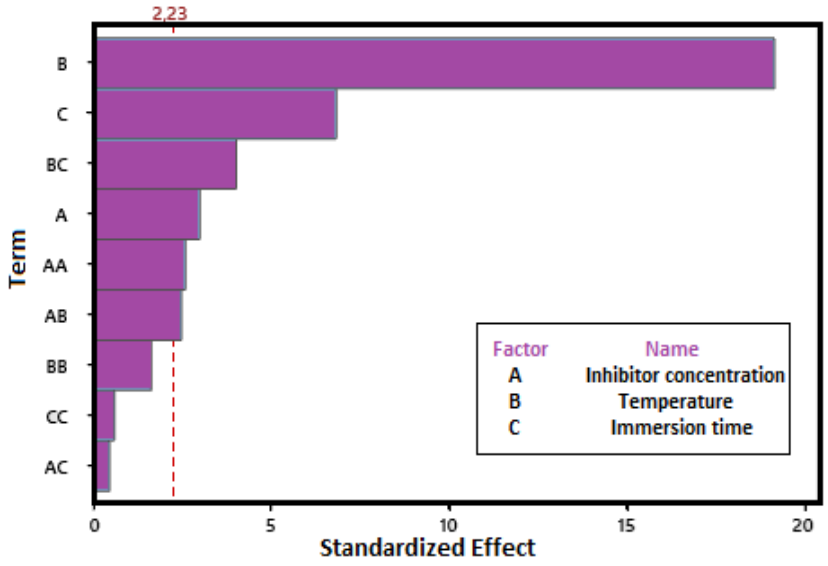

Figure 3. Pareto chart for the standardized effects of inhibitor concentration, temperature, and immersion time on the corrosion current density of tin in an acidic environment

The Pareto chart reveals which effects are important since it displays the absolute value of effects, but it does not determine which effects raise or reduce the response. Using Standardized Effects, The Normal probability plot (Figure 4) helps investigate the magnitude and direction of the impacts on a graph. The normal plot in Figure 4 indicates that the concentration of olive leaf extract and its interaction with temperature have a negative standardized effect, indicating that when the concentration of extract used increases from low to high level, the rate of corrosion decreases. The principal effects of temperature and immersion duration, on the other hand, have positive standardized effects.

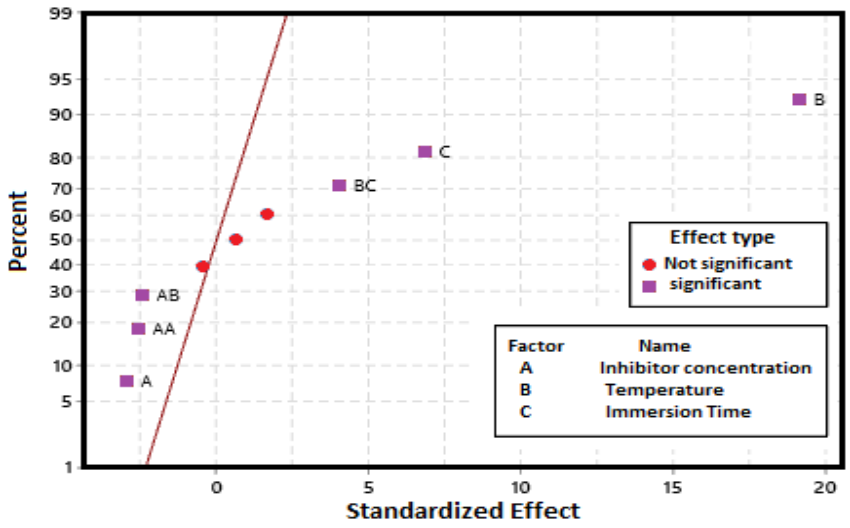

Figure 4. Normal plot of the standardized effects of inhibitor concentration, temperature, and immersion time on (i_{corr})

It is also necessary to calculate the effects and interactions of the variables. In this case, the value of P is the most important measurement; all parameters have a significant impact on the corrosion current density when their p-value is less than 0.05 [25]. The p-value of the squared effect of temperature is 0.133, the squared effect of immersion time is 0.567 and the interaction between extract concentration and immersion time is 0.655, which are inefficient model terms as shown in Table 5. However, because the p-value of the model in Table 5 is 0.000, deleting them is unneeded. From the three elements examined in this research, it can be stated that the effect of extract concentration is weak, however temperature has a significant influence on the rate of corrosion of tin in an acid medium.

Table 5. Calculated coded coefficients for corrosion current density (i_{corr})

Factor	**Coefficient**	**Standard Error Coefficient**	**T-Value**	**P-Value**
Constant	48.85	1.61	30.38	0.000
Inibitor concentration	-4.42	1.48	-2.99	0.014
Temperature	28.35	1.48	19.17	0.000
Immersion time	10.12	1.48	6.84	0.000
inhibitor*inhibitor	-7.29	2.82	-2.59	0.027
temperature*temperature	4.61	2.82	1.64	0.133
immersion time* immesrion time	1.67	2.82	0,59	0.567
inhibitor*temperature	-4.10	1.65	-2,48	0.033
inhibitor*immersion time	-0.76	1.65	-0,46	0.655
temperature*immersion time	6.66	1.65	4,03	0.002

3.5. Response surface plotting of the experimental conditions

3.5.1. Interactive effect of inhibitor concentration (g/L) and temperature (°C)

The acquired outcomes were shown employing a contour plot and response surface plot (3D). Figure 5 shows 3D charts exhibiting the effects of inhibitor concentration and temperature on (i_{corr}) during predefined conditions. The figure below demonstrates that with a hold value of 6.25 h for immersion time, the effect of temperature increased significantly the corrosion current density from 12 µA/cm² to 98 µA/cm². However, (i_{corr}) appeared to have very tiny fluctuation in value as the inhibitor concentration value enhanced; indicating that, in comparison to temperature, the inhibitor concentration had little effect on the response. Nevertheless, several other investigations have revealed that inhibitors have a considerable effect on inhibitory activity regardless of temperature [25,32].

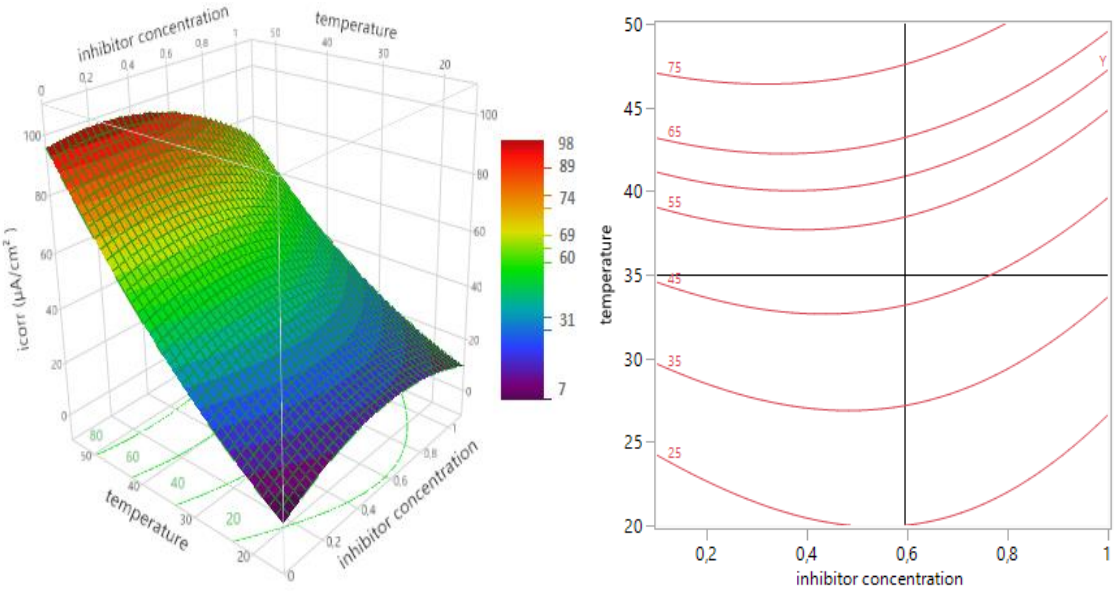

Figure 5. Response surface and contour plots illustrating the effect of inhibitor concentration and temperature on (i_{corr}) of tin in an acidic environment

3.5.2. Interactive effect of immersion time (h) and inhibitor concentration (g/L)

The response surface and contour plots for the influence of immersion time and inhibitor concentration on (i_{corr}) are presented in Figure 6. With a hold level of temperature (35°C), the corrosion current density increased gradually as immersion duration increased, from 27 to 69 µA/cm². There was a minor fluctuation in corrosion current density as extract content increased. As a result, the response variance associated with the inhibitor concentration was still considered to be quite minimal.

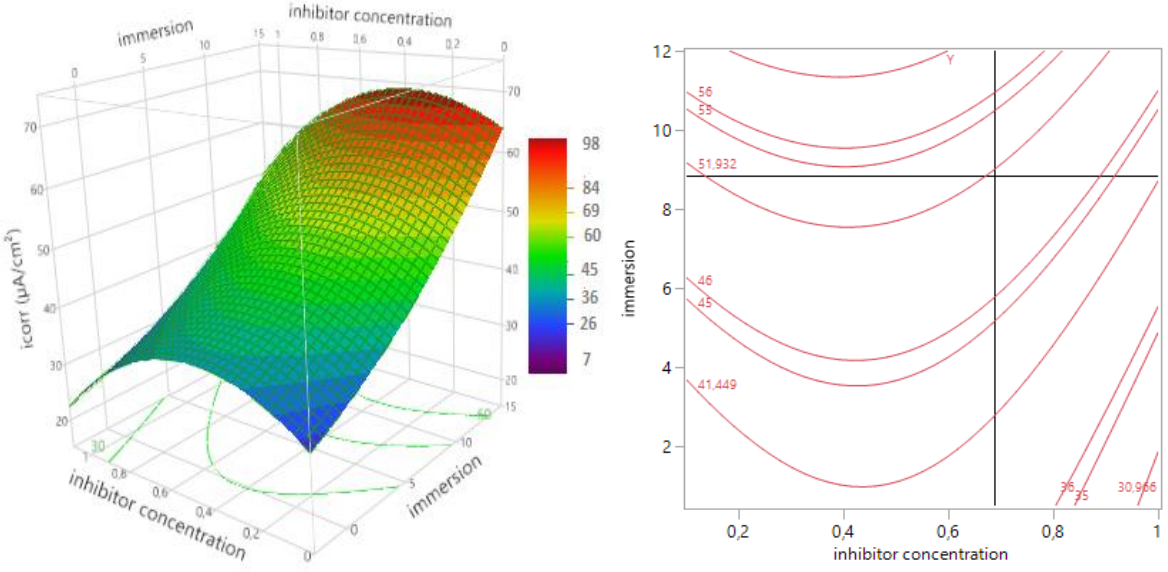

Figure 6. Response surface and contour plots illustrating the effect of inhibitor concentration and immersion time on (i_{corr}) of tin in an acidic environment

3.5.3. Interactive effect of temperature (°C) and immersion time (h)

The influence of immersion duration and temperature on (i_{corr}) is depicted in Figure 7. At a hold value of 0.55 g/L for extract concentration, an increase in temperature was related with an increase in corrosion current density of tin in 3 w% of acetic acid. From lowest to highest values of temperature, the corrosion current density enhanced from 19 to 82µA/cm², indicating a significant influence. Meanwhile, in this interaction case, as immersion time rises, the corrosion current density remains practically unchanged.

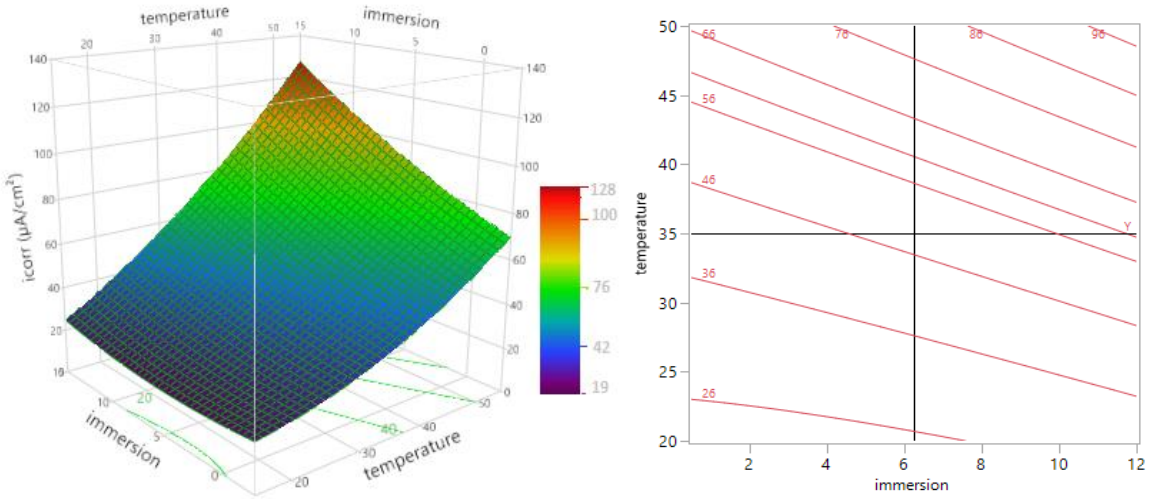

Figure 7. Response surface and contour plots illustrating the effect of temperature and immersion time on (i_{corr}) of tin in an acidic environment

3.6. Inhibition mechanism

Although some researchers have presented olive leaf extract as an effective green corrosion inhibitor [34-38] , to the best of our knowledge, no one has tested it as a tin corrosion inhibitor in a 3% acetic acid media. Numerous investigations have explored the existence of a variety of phenolic compounds in this extract, including hydroxytyrosol, oleuropein, rutin, luteolin-7-glucoside and verbascoside [37,38]. Oleuropein is the most prevalent component, as reported by various publications [34,36]. The molecular structures of oleuropein are depicted in Figure 8 [34].

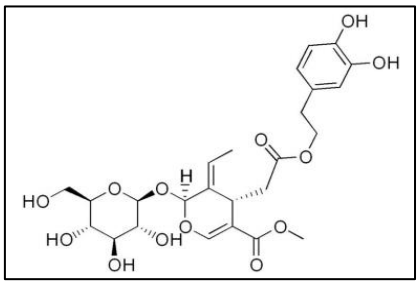

Figure 8. Chemical structure of oleuropein

According to the results of the PDP experiment, Olive leaves extract inhibits the corrosion action of tin in 3% acetic acid solution, which can be defined on the adsorption operation [35]. As a result, olive leaf extract molecules were adsorbed on the tin surface, creating a barrier film that inhibits the attack of CH_3COOH (H^+, CH_3COO^-) ions and water. Adsorption can be represented by two fundamental types of reactions: chemisorption and physisorption. In our case the increase of the corrosion current density with the temperature implies that physisorption is the primary process. This type of inhibitor is efficacious at room temperature, but lose their inhibitory performance at higher temperatures [38]. As previously stated, this extract is composed of a variety of natural organic compounds with many heteroatoms, π site in functional groups (C-O, O-H, N-H, C=O) and O-heterocyclic rings [36]. When the compounds of this inhibitor are added to an acidic medium, they get protonated, and are physically adsorbed on the tin surface through electrostatic interaction with CH_3COO^-. In addition, the inhibitory effect of this extract can be attributed to the adsorption through the synergistic effect of the predominant components as well as the minor elements of the inhibitor's composition [39].

4. CONCLUSION

In this investigation the effects of immersion time, temperature, and olive leaves extract as a green inhibitor on the corrosion behavior of a pure tin in an acidic media (3wt% acetic acid) were studied by statistical method RSM with FCCD. The study's findings indicate that the temperature and duration of immersion have a negative impact on the response, but the concentration of inhibitor serves to reduce the density of the corrosion current. An efficient statistical model has been developed to investigate methods of protecting tin packaging. It was revealed that the level of influence of independent factors on corrosion rate follows a rising sequence of inhibitor concentration immersion time then temperature. Since temperature was the most critical parameter impacting corrosion, more research with larger temperature ranges is required.

Conflict of Interest

The authors declared that there is no conflict of interest.

REFERENCES

[1] G.Kr. Deshwal, and N.R. Panjagari, J. Food Sci. Technol. 57 (2020) 2377.

[2] R. Lm, D. Lf, S. Ag, G. Em, M. Jof, T. Cg, and T. Ha, Integr Food Nutr. Metab. 5 (2018).

[3] R. Nabah, H. Lgaz, H. Zarrok, M. Larouj, F. Benhiba, K. Ourrak, M. Cherkaoui, A. Zarrouk, R. Touir, and H. Oudda, J. Mater. Environ. Sci. 8 (2017) 3730.

[4] J. Halambek, I. Cindrić, and A. Ninčević Grassino, Carbohydr. Polym. 234 (2020) 115940.
[5] B.V. Salas, M.S. Wiener, J.M. Bastidas, J.R. Salinas Martínez, and G.L. Badilla, Reference Module in Food Science. (2016) B9780081005965031000.
[6] S. Featherstone, A Complete Course in Canning and Related Processes. (2015) pp. 75–117.
[7] S. Blunden, and T. Wallace, Food Chem. Toxicol, 41 (2003) 1651.
[8] I.N. Pasias, K.G. Raptopoulou, and C. Proestos, Reference Module in Food Science. (2018) B9780081005965226000.
[9] A. Boumezzourh, M. Ouknin, E. Chibane, J. Costa, A. Bouyanzer, B. Hammouti, and L. Majidi, Int. J. Corros. Scale Inhib, 9 (2020).
[10] X. Zheng, D. Xia, H. Wang, and C. Fu, Anti-Corros. Method 60 (2013) 153.
[11] B. EL Ibrahimi, L. Bazzi, and S. EL Issami, RSC Adv. 10 (2020) 29696.
[12] D. Zhou, J. Wang, Y. Gao, and L. Zhang, Int. J. Electrochem. Sci. (2017) 192.
[13] B.M.C. Soares, C.A.R. Anjos, T.B. Faria, and S.T. Dantas, Packag. Technol. Sci. 29 (2016) 65.
[14] S. Dey, and B.H. Nagababu, Food Chem. Adv. 1 (2022) 100019.
[15] C. Melvin, E. Jewell, J. Miedema, K. Lammers, A. Vooys, A. Allman, and N. McMurray, Packag Technol Sci. 32 (2019) 345.
[16] S. Noureddine El Moussawi, R. Karam, M. Cladière, H. Chébib, R. Ouaini, and V. Camel, Food Addit. Contam. 35 (2018) 377.
[17] B. El Ibrahimi, A. Baddouh, R. Oukhrib, S. El Issami, Z. Hafidi, and L. Bazzi, Appl. Surf. Scis. 23 (2021) 100966.
[18] D.T. Oyekunle, T.I. Oguntade, C.S. Ita, T. Ojo, and O.D. Orodu, Mater. Today Commun. 21 (2019) 100691.
[19] D.-I. Vaireanu, A. Cojocaru, I. Maior, and I.-A. Ciobotaru, Reference Module in Food Sci. (2018) B9780081005965224000.
[20] F.O. Edoziuno, A.A. Adediran, B.U. Odoni, A.D. Akinwekomi, O.S. Adesina, and M. Oki, Cogent Eng. 7 (2020) 1714100.
[21] Y. Elkhotfi, H. Boubekraoui, J. Zoubir, I. Forsal, and E. Rakib, J. Chem. Technol. Metall. 56 (2021) 174.
[22] Y. Elkhotfi, M.E. Ghozlani, Y. Hakamaoui, I. Forsal, E.M. Rakib, and B. Mernari, Am. J. Eng. Res. 6 (2017) 247.
[23] N.T. Chung, Y.S. So, W.C. Kim, and J.G. Kim, Mater. 14 (2021) 6596.
[24] P.R. Prabhu, D. Prabhu, and P. Rao, J. Mater. Res. Technol. 9 (2020) 3622.
[25] A.A. Dastgerdi, A. Brenna, M. Ormellese, M. Pedeferri, and F. Bolzoni, Corros. Sci. 159 (2019) 108160.
[26] W. Wang, Y. Cheng, and G. Tan, Mater. 11 (2018) 1311.

[27] A. Fenech, T. Fearn, and M. Strlic, Polym. Degrad. Stab. 97 (2012) 621.
[28] C.A. Gervasi, P.A. Palacios, M.V. Fiori Bimbi, and P.E. Alvarez, J. Electroanal. Chem. 639 (2010) 141.
[29] M. Ahmadi, K. Rahmani, A. Rahmani, and H. Rahmani, Polish J. Chem. Technol. 19 (2017) 104.
[30] S. Bhattacharya, and P. Kayaroganam (Ed.), Intech Open (2021).
[31] G. Di Leo, and F. Sardanelli, Eur. Radiol. Exp. 4 (2020) 18.
[32] O. Olawale, J.O. Bello, B.T. Ogunsemi, U.C. Uchella, A.P. Oluyori, and N.K. Oladejo, Heliyon 5 (2019) 02821.
[33] I. Forsal, M.E. Touhami, B. Mernari, J. El-Hajri, and M.F. Baba, Port. Electrochim. Acta 28 (2010) 203.
[34] B. Mohammed, and T.A. Salman, Plant Arch. 20 (2020) 7089
[35] H.M. Elabbasy, and A.S. Fouda, Green Chem. Lett. Rev. 12 (2019) 332.
[36] D. Bouknana, B. Hammouti, H. Serghini caid, S. Jodeh, A. Bouyanzer, A. Aouniti, I. and Warad, Int. J. Ind. Chem. 6 (2015) 233.
[37] M. Ben Harb, S. Abubshait, N. Etteyeb, M. Kamoun, and A. Dhouib, Arab. J. Chem. 13 (2020) 4846.
[38] C. Rahal, M. Masmoudi, R. Abdelhedi, R. Sabot, M. Jeannin, M. Bouaziz, and P. Refait, J. Electroanal. Chem. 769 (2016) 53.
[39] M. Boudalia, R. M. Fernández-Domene, M. Tabyaoui, A. Bellaouchou, A. Guenbour, and J. García-Antón, J. Mater. Res. Technol. 8 (2019) 5763.